Irregular Wave Dissipation by Coastal Vegetation

Basic Information

Title:	Irregular Wave Dissipation by Coastal Vegetation
Project Number:	2012LA87B
Start Date:	3/1/2012
End Date:	2/28/2012
Funding Source:	104B
Congressional District:	6th
Research Category:	Climate and Hydrologic Processes
Focus Category:	Sediments, Geomorphological Processes, Wetlands
Descriptors:	None
Principal Investigators:	Heather Smith

Publications

There are no publications.

Project Title: Irregular Wave Dissipation by Coastal Vegetation
Start Date: March 1, 2012
End Date: February 28, 2013
Funding Source: 104B
Congressional District: 6
Research Category: Coastal Engineering - Water Resources
Focus Categories: SED, G&G, WL
Keywords: Waves, vegetation, wetlands, turbulence
Principal Investigator: Heather D. Smith

Problem Description

The role of natural coastal defenses in reducing damage from extreme events is a topic of high importance. Events such as the 2004 Indian Ocean Tsunami, Hurricanes Katrina and Rita in 2005, and more recently, Hurricane Sandy in 2012, have continued to illustrate the need for better coastal defenses, and perhaps more importantly, development of accurate predictive models to aid in local evacuation and emergency response planning. Natural coastal defenses include barrier islands, wetlands, and shoals. The sustainability of these regions and therefore their populations and resources, will continue to be an engineering problem for the foreseeable future.

In the planning of coastal restoration projects, wetlands have been identified as desirable due to their buffer capabilities, pasticularly for reducing storm surge and wave impact. While preliminary data may indicate that the presence of vegetation does reduce wave height, the available data is rather sparse and the actual mechanism for wave reduction is not yet understood. Observations in mangroves by Mazda *et al.* (1997) showed a reduction of wave height from 1.0 m at the front edge of the forest to 0.05 m at the coast for older and denser forests. Newer plantings showed minimal wave reduction. Möller (2006) observed wave attenuation in salt marshes at a variety of depths and wave heights. When the relative wave height (wave height over water depth) became large enough, wave reduction became negligible. Wave attenuation was also small in larger depths where the vegetation was submerged. Wave attenuation was also spatially and seasonally variable, with a dependence on the amount of vegetation cover. Newell and Koch (2004) also observed this dependency of vegetation cover with seagrasses, as no appreciable wave attenuation was observed until the density of the seagrass passed some threshold. The seasonal cycle of the seagrass was also investigated. During the vegetative period, plants are shorter and extend only partially through the water column. This results in a significant decrease in the wave attenuation observed during reproductive periods where the grass extends through most of the water column or is emergent.

A variety of physical experimentation has been performed to investigate fluid-vegetation interactions and estimate the drag coefficient. In studies of emergent vegetation in steady current, Nepf (1999) proposed a cylinder based model where the bulk drag coefficient for the vegetation was calibrated with laboratory data and the influence of plant density and cylinder configuration were examined for Reynolds numbers (UD/ν) of 4,000-10,000. Tanino and Nepf (2008) extended the range of this work by increasing plant density and the range

of the Reynolds number. Of particular interest were Reynolds numbers less than 700, where individual cylinder wake interactions are reduced. The bulk drag coefficient was found to decrease with increasing Reynolds number and solid volume fraction.

In wave environments, Dalrymple *et al.* (1984) proposed a formulation to model the energy dissipation provided by an array of cylinders and the resultant reduction of the wave height. The decay formulation follows

$$K = \frac{H(x)}{H_0} = \frac{1}{1 + \alpha x} \tag{1}$$

where H_0 is the incoming wave height and $H(x)$ is the wave height at location x into the vegetation. The damping factor, α, is given by

$$\alpha = \frac{g^2 C_d N D H_0}{9\pi k c_g c^3} \frac{\left(\cosh^2(kl_v) + 2\right) \sinh(kl_v)}{\cosh^3(kh)} \tag{2}$$

where g is graity, C_d is the drag coefficient, N is the stem density, D is the stem diameter, k is the wavenumber, l_v is the vegetation height, or the water depth, whichever is smaller, h is the water depth, c_g is the wave group velocity, and c is the group velocity. Several authors (e.g. Augustin *et al.* (2009) and other unpublished works) have utilized this formulation to investigate the relationship of hte bulk drag coefficient with other hydrodynamic parameters, including the Reynolds number ($Re = U_w D/\nu$) and Keulegan-Carpenter number ($KC = U_w T/D$) where T is the wave period and U_w is some wave velocity scale often assumed as the maximum velocity. It has been found that the drag coefficient has a higher correlated relationship with Keulegan-Carpenter number.

The wave height decay formularion can also extended for irregular waves (Mendez and Losada, 2004),

$$K = \frac{H_{rms}(x)}{H_{rms,0}} = \frac{1}{1 + \beta x} \tag{3}$$

where the root-mean-squared (rms) wave heights are utilitized. The decay function, β, has a similar form as α in equation (1),

$$\beta = \frac{1}{3\sqrt{\pi}} C_d D N H_{rms,0} \frac{\sinh^3(kl_v) + 3\sinh(kl_v)}{(\sinh(2kh) + 2kh)\sinh(kh)} \tag{4}$$

In this case, the wavenumber, k, is determined using the peak period, T_p, of the irregular waves.

Methodology

During the summer of 2010, PI Smith and her graduate students participated in a NSF-funded experiment at the O. H. Hinsdale Wave Research Laboratory at Oregon State University. The original study "Ecological modeling of emergent vegetation for sustaining wetlands in high wave energy coastal environments" was proposed by Dr. Daniel Cox and Dr. Denny Ablert at Oregon State University. LSU's participation was supported by the Louisiana Board of Regents and the Louisiana Water Resources Research Institute. The experiment was performed in the Large Wave Flume, which is 104 m long, 3.7 m wide, and 4.6 m deep.

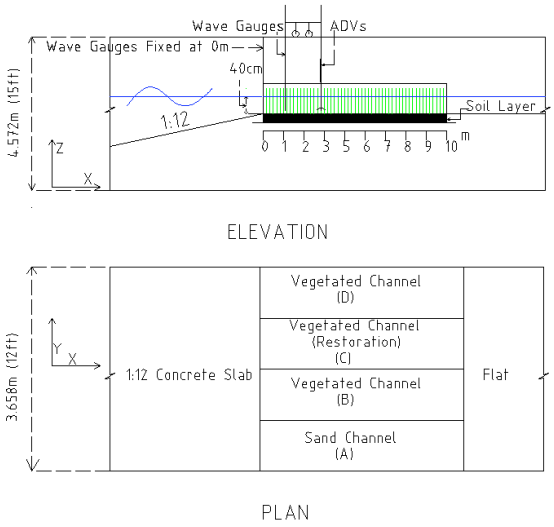

Figure 1: Experimental setup in the Large Wave Flume. Figure is not to scale.

The flume was divided into four, 10 m long channels as shown in Figure 1(a). Three of the four channels were planted with bulrush (*Schoeneplectus pungens*), which is a fairly common species of wetland vegetation growing throughout the United States. Bulrush is a perennial species with the stem having a triangular cross-section for most of the upper part with a circular cross-section at the base. The vegetation used in the experiment were harvested from young natural bulrush beds in the Tillamook Bay of Oregon in the late spring of 2009. The bulrush stems with their root system still intact were cut out in blocks from the inner estuarine regions experiencing low to moderate wave forcing similar to what was simulated in the laboratory. These were then placed in the specially constructed channel boxes and careful preparation was undertaken to sustain their growth throughout the winter of 2009 in the laboratory. The purpose of this exercise was to mimic the field conditions in the best possible way. Channel A was the control sand channel. Channel B had a vegetation density of 1,256 stems/m^2, Channel C had a vegetation density of 999 stems/m^2, and channel D had a density of 1,219 stems/m^2. The majority of the stems in the channel were taller than the location of the free surface. After the initial experiments, the vegetation in channel D was thinned to approximately 630 stems/m^2.

Wave gauges were placed at the leading edge of each channel and on a moveable platform. This allowed for the observation of the free surface at a variety of locations within the channels. During the three-week experiment, over 200 wave trials were run for the measurement of wave attenuation, and nearly 100 wave trials were run for the investigation of the velocity and turbulence characteristics within the vegetation. The results descibed here are for wave runs with a 40 cm water depth, leading to fully emergent vegetation. Wave heights of 5-20 cm and wave periods of 1-3 s were considered, which are typically of estuarine waves.

Results

Figure 2 presents the decay curves for the wave height through the vegetated channels. In this figure, the symbols are the laboratory obtained data, while the dashed lines of corresponding color are the best fit curve using Equations (1) for regular waves and (3) for irregular waves. The top panel shows the observations from channel B. The first two runs (blue

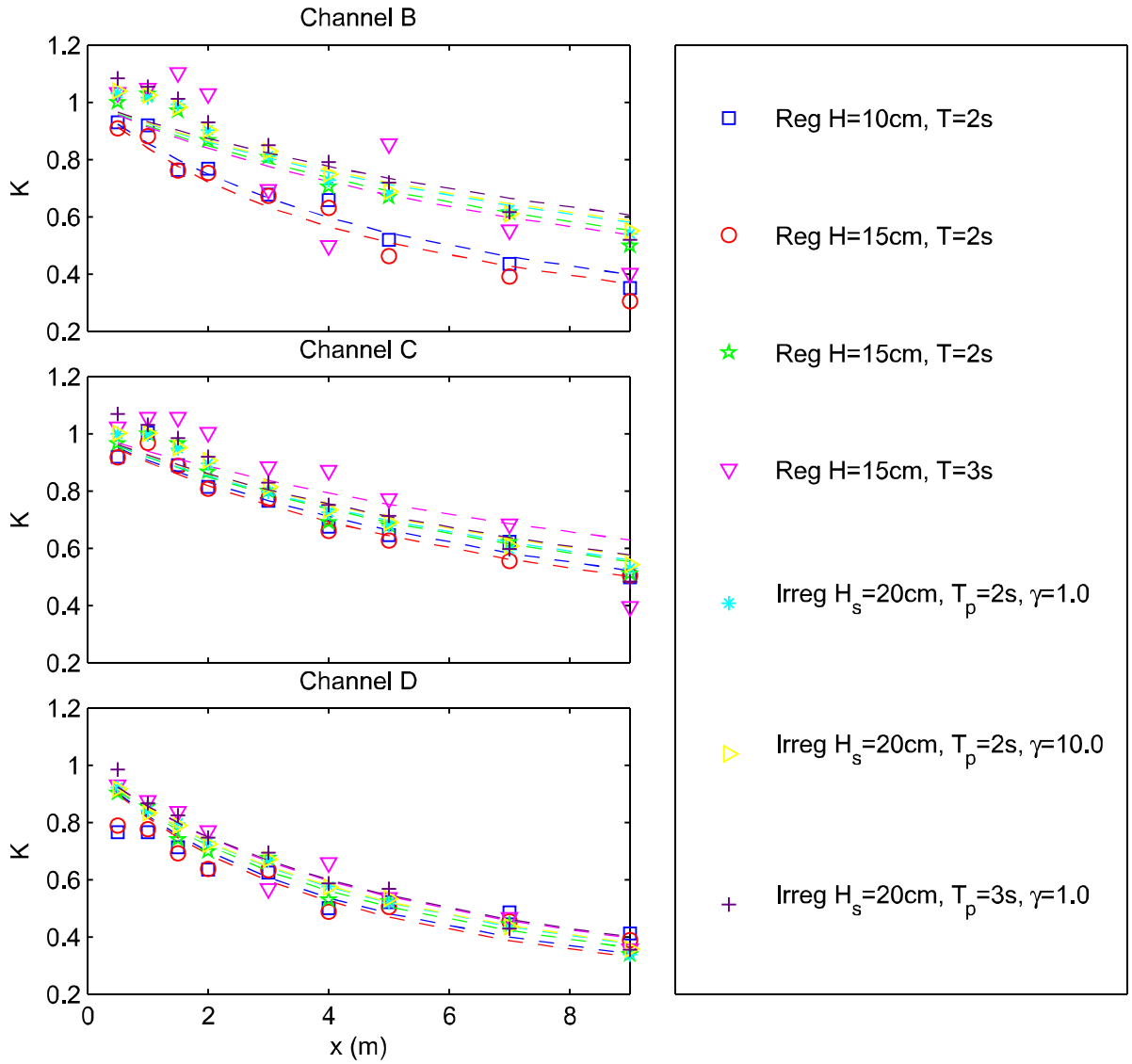

Figure 2: The decay of the wave height $K = H/H_0$ for the vegetated channels for regular and irregular waves.The observations are the symbols and the dashed lines are the best fits using Equations (1) for regular waves and (3) for irregular waves.

squares and red circles) were obtained at the original vegetation density of 1,256 stems/m^2. The remaining runs were obtained at a roughly 50% lesser density of 630 stems/m^2. The effect of the different vegetation density is quite marked with a much greater decay with the higher vegetation density. For the remaining panels (Channels C and D), the differences in the two cases for a regular two second wave with an incoming wave height of 15 cm (red circles and green stars) should be similar. In Channels C and D, a small difference in the decay in these two cases is observed. This variation is due to the state of the plant stem. The initial case (red circles) was obtained at the beginning of the experiment, whereas the latter case (green stars) was obtained a week later near the end of the experiment. As the experiment progressed, the stem stiffness reduced due to the combination of repeated wave action and the lack of direct natural light for the plants in the laboratory. The reduced

	α				β		
H_o	10	15	15	15	20	20	20
T	2	2	2	3	2, $\gamma = 1.0$	2, $\gamma = 10.0$	3, $\gamma = 1.0$
γ	N/A	N/A	N/A	N/A	$\gamma = 1.0$	$\gamma = 10.0$	$\gamma = 1.0$
Chan. B	0.168	0.193	0.090	0.096	0.081	0.076	0.072
Chan. C	0.102	0.111	0.090	0.066	0.087	0.083	0.082
Chan. D	0.216	0.226	0.196	0.171	0.185	0.183	0.168

Table 1: Decay coefficients from the best fit lines using Equations (1) for regular waves and (3) for irregular waves.

stem stiffness results in a lesser decay of the waves through the channel. A slight period dependency can be observed, with the smaller period waves decaying more through the vegetation. This is observed for both the regular and irregular wave cases. The effect of the differing wave height is also presented for a 10 cm and 15 cm wave with a period of 2 s. The larger waves show a greater decay in the channel, although the amount of the difference varies from channel to channel.

The irregular wave action can be compared with that of regular waves. The decay for the irregular waves as a given period and is a little larger than for the comparable regular wave case. This may be due to the larger wave height (20 cm) for the irregular waves. Within the irregular waves, the effect of spectral spread parameter ($\gamma = 1.0$ or $\gamma = 10.0$) is small.

Table 1 compares the decay coefficients of the best fit line using Equations (1) for regular waves and (3) for irregular waves. As shown in Figure 2, the effect of the plant density is large. A 50% reduction in plant density (channel B, cases 2 and 3) results in a roughly 50% redcution in the decay coefficient α. This is consistent with Equation (2) in which the stem density N is directly proportional to α. The effect of density and stem height is shown between channels C and D. Channel D had a more consistent and higher stem height than channel C due to the planting nature of the restoration-type planing used in channel C. While the expected reduction in decay vaules for both α and β due only to different density is around 20%, the decay coefficients actually reduce by around 50%. This is consistent over all of the regular and irregular wave cases.

For irregular waves, the variation of the temporal spectra and wave height distribution across the channel is necessary. Figure 3 presents the 2 s, $\gamma = 1.0$ wave height distribution (top panels) and temporal spectra (bottom panels) across channel D (left to right). Figure 4 presents the 2 s, $\gamma = 10.0$ wave case, and Figure 5 presents the 3 s, $\gamma = 1.0$ wave case. At the beginning of the channel (left panel), the wave height distribution is wide. The blue line is the best fit Rayleigh distribution, which most accurately describes wave height disctriubtions. As the waves progress down the channel, the larger wave heights are reduced. As the number of waves in the channel does not change, this results in a shifting of the distribution toward lower wave heights and a steepening of the distribution. Interesting, the Rayleigh distribution continues to fit the observations reasoonably well. The exception to this is the peakier distribution obtained with a spectral spread parameter ($\gamma = 10.0$). In this case, the peak of the distribution is not well described with the Rayleigh distribution. In each panel, the significant wave height, H_s, is presented and represents the average of the highest one-third of the waves.

The influence of the spactral spread parameter, γ, and the change in peak period can bc analyzcd with thc bottom pancls of thc Figurcs. A spcctral sprcad paramctcr of $\gamma = 1.0$ results in a wider spectra that is more consistent with locally generated waves in estuarine environments. The greater spectral spread parameter of $\gamma = 10.0$ results in a sharper spectra more consistent with offshore generated storm waves. The highest peak in the spectra is the location of the peak period, T_p. The location of the peak period does not change significantly between locations within the channel. The total energy within the spectra does decrease with distance into the channel. This results in a majority of the remaining spectral energy consilodating around the peak period. As a result of the consilidation of the wave energy around the peak period and the steepening of the wave height distribution, the waves are becoming more regular as they progress through the vegetation.

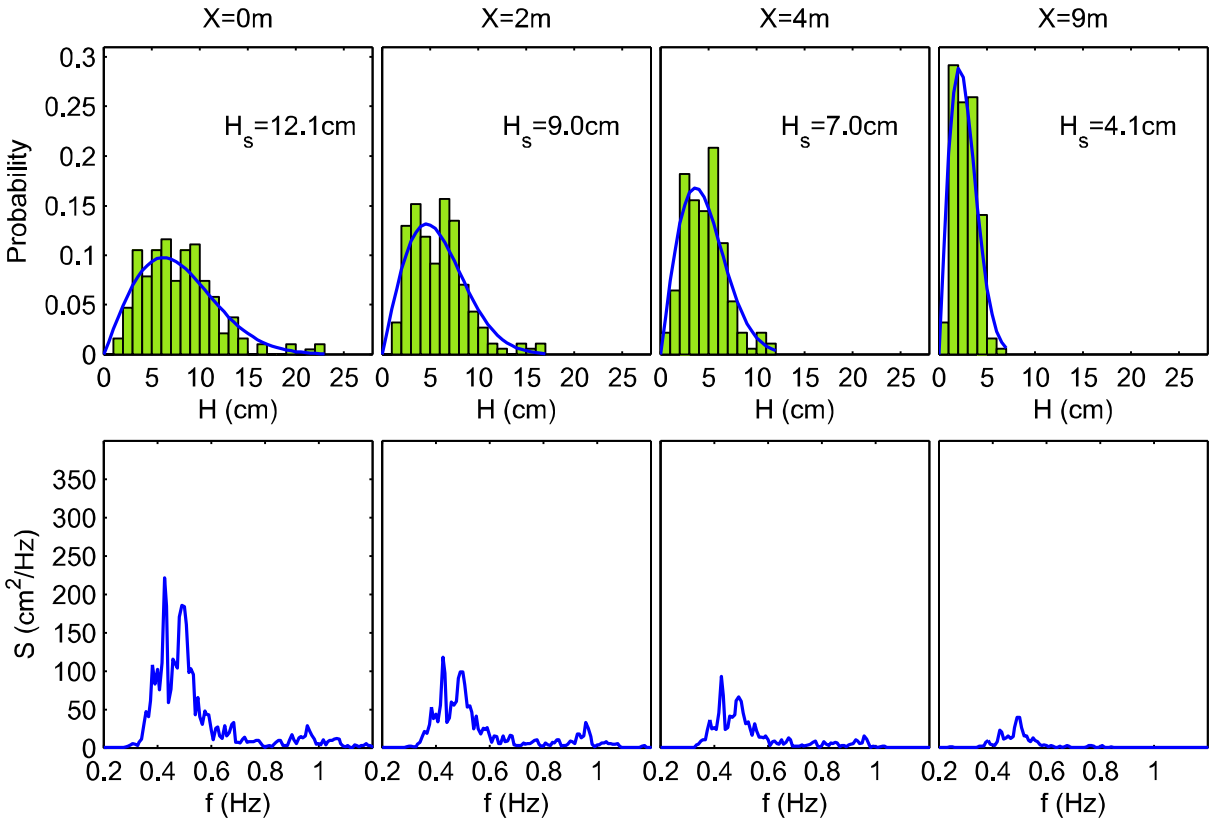

Figure 3: The wave height distribution (top panels) and temporal spectra (bottom panel) for the 2 s, 20 cm wave case with a spectral spread parameter of $\gamma = 1.0$.

Conclusions

Wetland vegetation is potentially significant solution to help mitigate storm generated waves along the coastline. As shown in this research, wave attenuation of upwards of 60% were observed within the first 10 m of a vegetated channel. The dependency of the amount of wavc attcnuation on a varicty of wavc and vcgctation characteristics arc tcstcd with livc vegetation in a controlled laboratory environment. As predicted by theory, the amount of damping is dependent on the density of the vegetation. A reduction of the vegetation density

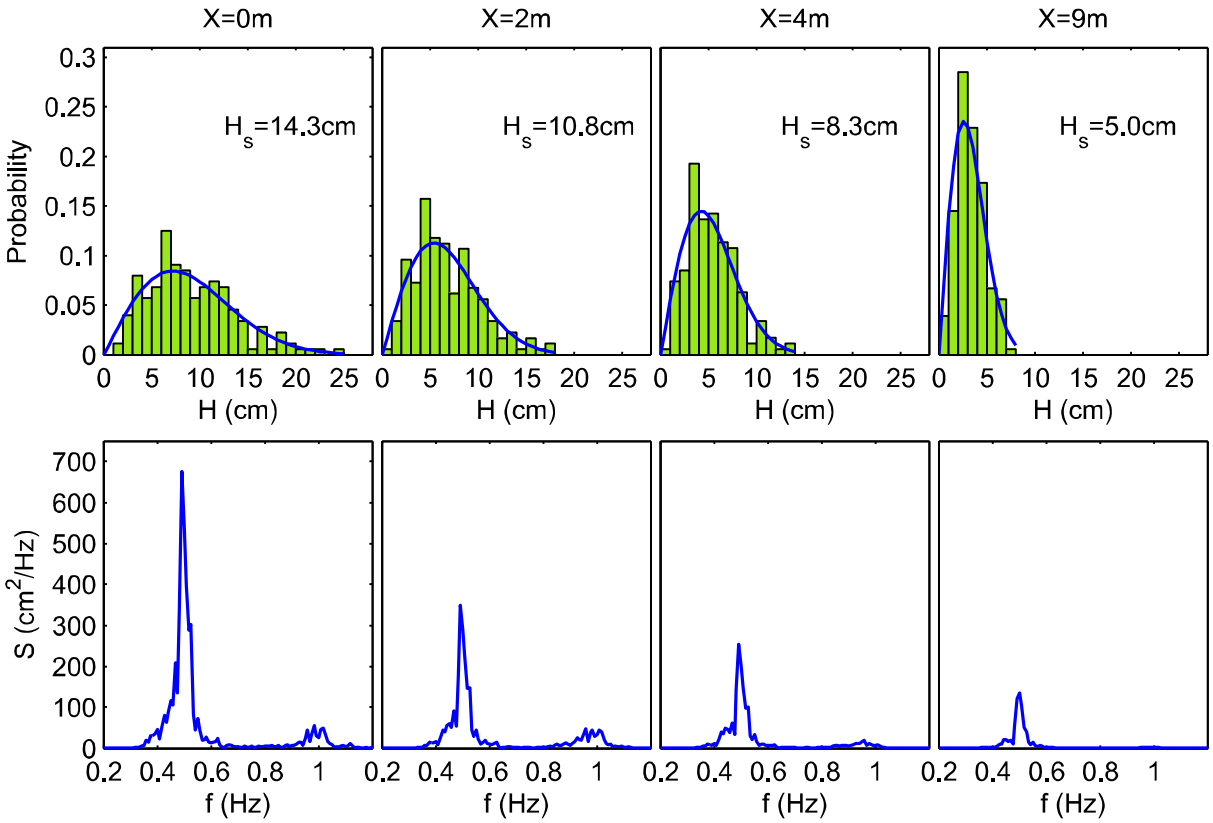

Figure 4: The wave height distribution (top panels) and temporal spectra (bottom panel) for the 2 s, 20 cm wave case with a spectral spread parameter of $\gamma = 10.0$.

of 50% resulted in a reduction in the dampening capability of the vegetation by 50% as well. Additionally, the stiffness of the plant itself can also be a contributing factory to the amount of dissipation provided. However, the mechanism for including these factors is imperfect and is lumped into the drag coefficient, C_d. This presents a difficulty for researchers utilizing these theoretical models, as the same vegetation patch may have a different performance depending on these hard to quantify plant characteristics. The consistency of the height of the vegetation was also shown to have an effect. Consistently higher stems produced more dissipation than those with a greater stem variability, like newly planted restoration wetlands.

In terms of wave characteristics, lower wave periods were shown to be more susceptible to damping. Waves with a greater wave height were shown to decay more through the vegetation. In our study irregular waves showed slightly greater decay than a similarly sized regular wave field. However, it is unclear if this increased decay is due to the irregular nature of the waves, or to the wave height for the irregular waves being 5 cm larger. Irregular waves were found to continue to fit the Rayleigh distribution reasonably well throughout the vegetation. The exception to this was the wave case with a well defined and sharp spectrum. In this case, the Rayleigh distribution does not match as well at any point, including the incoming wave field at the upstream edge of the vegetation. Due to the preferential damping of the larger waves, the wave heights are reduced and tend move towards a regular wave

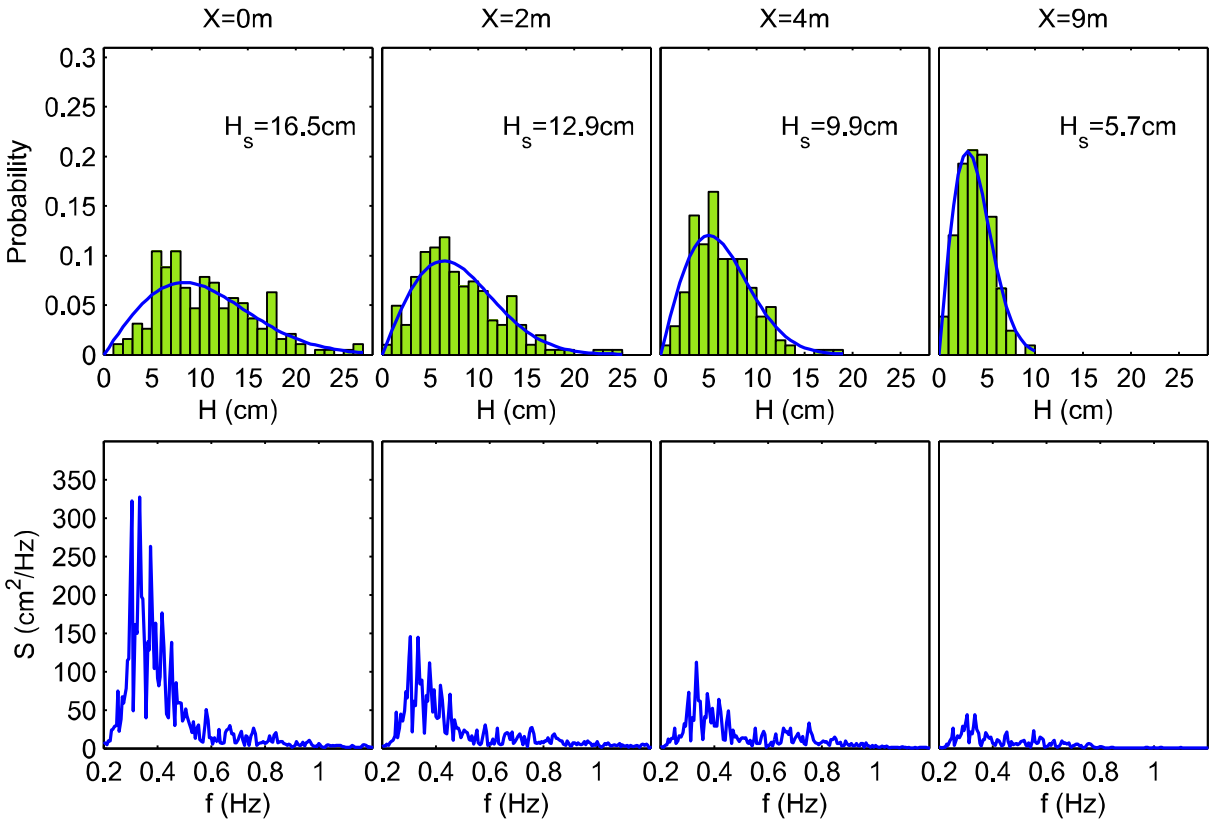

Figure 5: The wave height distribution (top panels) and temporal spectra (bottom panel) for the 3 s, 20 cm wave case with a spectral spread parameter of $\gamma = 1.0$.

field. The peak period did not show any significant changes through the vegetation.

References

Augustin, L. N., Irish, J. L., and Lynett, P. (2009). Laboratory and numerical studies of wave damping by emergent and near-emergent vegetation. *Coast. Eng.*, 56(3):332–340.

Dalrymple, R. A., Kirby, J. T., and Hwang, P. A. (1984). Wave diffraction due to areas of energy dissipation. *J. Waterw., Port, Coastal, Ocean Eng., ASCE*, 110(1):67–79.

Mazda, Y., Magi, M., Kogo, M., and Hong, P. N. (1997). Mangroves as a coastal protection from waves in the Tong King delta, Vietnam. *Mangroves and Salt Marshes*, 1(2):127–135.

Mendez, F. J. and Losada, I. J. (2004). An empirical model to estimate the propagation of random breaking and nonbreaking waves over vegetation fields. *Coast. Eng.*, 51(2):103–118.

Möller, I. (2006). Quantifying saltmarsh vegetation and its effect on wave height dissipation: Results from a UK East coast saltmarsh. *Est. Coast. Shelf Sci.*, 69(3-4):337–351.

Nepf, H. M. (1999). Drag, turbulence, and diffusion in flow through emergent vegetation. *Water Resour. Res.*, 35(2):479–489.

Newell, R. I. E. and Koch, E. W. (2004). Modeling seagrass density and distribution in response to changes in turbidity stemming from bivalve filtration and seagrass sediment stabilization. *Estuaries*, 27(5):793–806.

Tanino, Y. and Nepf, H. M. (2008). Laboratory investigation of mean drag in a random array of rigid, emergent cylinders. *J. Hydraul. Eng., ASCE*, 134(1):34–41.